ANALYTICAL CONSTANT NODAL METHOD FOR MONOENERGETIC S_N EIGENVALUE PROBLEMS IN X,Y-GEOMETRY

Hermes Alves Filho and Fernando Carvalho da Silva
Universidade Federal do Rio de Janeiro
Programa de Engenharia Nuclear – COPPE
P.O. Box 68 509
21 945-970, Rio de Janeiro, RJ, Brazil
fernando@lmn.con.ufrj.br

Ricardo C. Barros
Universidade do Estado do Rio de Janeiro
Instituto Politécnico – IPRJ
P.O. Box 97 282
28 601-970, Nova Friburgo, RJ, Brazil
ricardob@iprj.uerj.br

ABSTRACT

We describe a hybrid spectral nodal method applied to one-speed S_N eigenvalue problems in X,Y-geometry for nuclear reactor global calculations. To solve the transverse-integrated S_N nodal equations, we generalize the spectral diamond (SD) method, that we developed for numerically solving slab-geometry S_N eigenvalue problems with no spatial truncation error. In the present generalization, we approximate the transverse leakage through the edges of each spatial node by constants, so we call our method the SD-constant nodal (SD-CN) method, that we use in the fuel regions of the nuclear reactor core. In the non-multiplying regions, e.g., reflector and baffle, we use the spectral Green's function-constant nodal (SGF-CN) method; hence the hybrid characteristic of our method. In order to converge the numerical solution for each S_N "fixed source" problem (inner iterations) in each outer iteration (power method), we use the one-node block inversion (NBI) scheme. We show some numerical results to a typical model problem to illustrate the method's accuracy to coarse-mesh calculations.

1. INTRODUCTION

Deterministic computational modeling of physical phenomena generally requires three major steps: (i) we need to use a mathematical model that usually consists of a set of differential equations, that supposedly represent approximately the physical phenomenon we want to analyze; (ii) we need to describe a convergent and accurate numerical scheme to approximate the

mathematical model we have settled in step (i); and (iii) we need to write an efficient algorithm to solve on a digital computer the discretized equations that we are left with by applying the numerical scheme, that we have settled in step (ii).

In this paper, we present a deterministic computational modeling of neutron transport for nuclear reactor global calculations (eigenvalue problem). We use the discrete ordinates (S_N) formulation[1] of the steady-state one-speed first order form of the neutron transport equation in X,Y-geometry as the mathematical model [cf. step (i)]. As with the numerical method [cf. step (ii)], practical limitations on computer storage and execution time have motivated the development of coarse-mesh methods for S_N problems. Therefore, we describe a hybrid spectral nodal method for coarse-mesh nuclear reactor S_N calculations. To solve the transverse - integrated S_N nodal equations, we generalize the spectral diamond (SD) method, that we developed for numerically solving slab-geometry S_N eigenvalue problems with no spatial truncation error.[2] In the present generalization, we approximate the transverse leakage through the edges of each spatial node by constants, so we call our method the SD-constant nodal (SD-CN) method [3], that we use in the fuel regions of the nuclear reactor core. In the non-multiplying regions, e.g., reflector and baffle, we use the spectral Green's function-constant nodal (SGF-CN) method [4]; hence the hybrid characteristic of the present SD-SGF-CN method. In order to converge the numerical solution for each S_N "fixed source" problem (inner iterations) in each outer iteration (power method), we use the one-node block inversion (NBI) iterative scheme [cf. step (iii)].[4]

At this point we present an outline of the remainder of this paper. In Sec. 2 we present the mathematical model. In Sec. 3 we describe the SD-CN method that we use in the fuel regions of the domain to form the present hybrid spectral nodal method. In Sec. 4 we describe the NBI iterative scheme. In conclusion, we present in Sec. 5 some numerical results and a brief discussion.

2. MATHEMATICAL MODEL

Let us consider the S_N equations in a rectangular domain D of width X and height Y with isotropic scattering

$$\mu_m \frac{\partial}{\partial x}\psi_m(x,y) + \eta_m \frac{\partial}{\partial y}\psi_m(x,y) + \sigma_T(x,y)\psi_m(x,y) = [\sigma_{S0}(x,y) + \frac{\nu}{k}\sigma_F(x,y)]\sum_{n=1}^{M}\psi_n(x,y)\omega_n + Q(x,y) \quad , \qquad (1)$$

where
$(x,y) \in D$, $m = 1:M$ with $M = N(N+2)/2$

N = order of the angular quadrature set
ψ_m = angular flux
σ_T = total macroscopic cross section
σ_{S0} = zero'th order component of the differential scattering cross section
σ_F = fission macroscopic cross section
k = eigenvalue
Q = isotropic neutron source in D
ν = average number of neutrons emitted in each fission event.

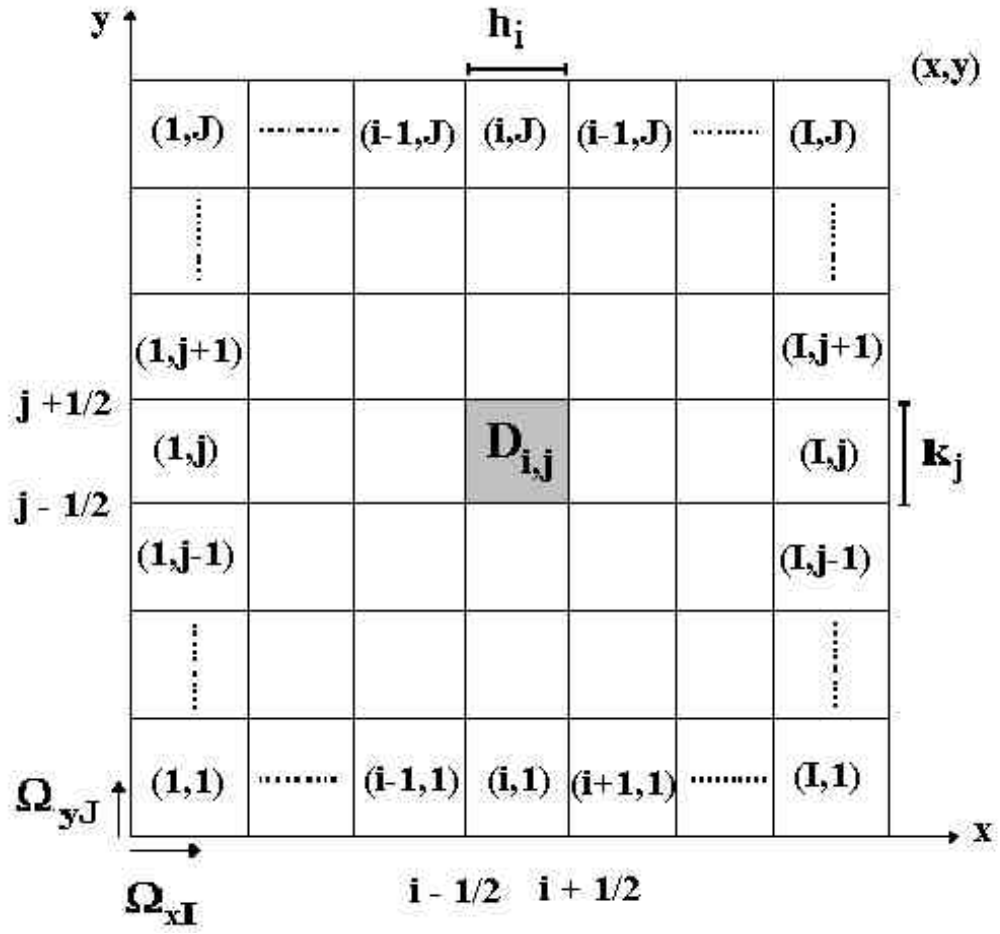

Figure 1. Spatial Grid Ω_{xI} x Ω_{yJ}.

At this point, let us consider an arbitrary spatial grid Ω_{xI} x Ω_{yJ} on D, where each spatial cell is termed node $D_{i,j}$ of width $h_i (i = 1:I)$ and height $k_j (j = 1:J)$, as shown in Figure 1. Each node $D_{i,j}$ has constant cross sections $\sigma_{Ti,j}, \sigma_{S0i,j}, \sigma_{Fi,j}$ and a constant interior source $Q_{i,j}$.

To obtain the one-dimensional transverse-integrated S_N nodal equations, we follow the standard procedure.[5] By applying the transverse integration operator

$$\frac{1}{k_j}\int_{y_{j-1/2}}^{y_{j+1/2}}(\circ)dy$$

to Eq. (1), we obtain the one-dimensional transverse-integrated S_N nodal equation for the x direction

$$\mu_m \frac{d}{dx}\tilde{\psi}_{m,j}(x) + \sigma_{Ti,j}\tilde{\psi}_{m,j}(x) = \tilde{S}_{m,j}(x) + Q_{i,j} - \frac{\eta_m}{k_j}[\psi_m(x, y_{j+1/2}) - \psi_m(x, y_{j-1/2})]. \quad (2)$$

Here we have defined the zero'th order y-moment of the angular flux

$$\tilde{\psi}_{m,j}(x) \equiv \frac{1}{k_j}\int_{y_{j-1/2}}^{y_{j+1/2}}\psi_m(x,y)dy \quad (3)$$

and similarly the zero'th order y-moment of the source

$$\tilde{S}_{m,j}(x) \equiv [\sigma_{S0i,j} + \frac{\nu}{k}\sigma_{Fi,j}]\sum_{n=1}^{M}\tilde{\psi}_{n,j}(x)\omega_n \quad . \quad (4)$$

Now we apply the transverse integration operator

$$\frac{1}{h_i}\int_{x_{i-1/2}}^{x_{i+1/2}}(\circ)dx$$

to Eq. (1) and we obtain the one-dimensional transverse-integrated S_N nodal equation for the y direction

$$\eta_m \frac{d}{dy}\hat{\psi}_{m,i}(y) + \sigma_{Ti,j}\hat{\psi}_{m,i}(y) = \hat{S}_{m,i}(y) + Q_{i,j} - \frac{\mu_m}{h_i}[\psi_m(x_{i+1/2}, y) - \psi_m(x_{i-1/2}, y)] \quad , \tag{5}$$

where we have defined the zero'th order x-moment of the angular flux

$$\hat{\psi}_{m,i}(y) \equiv \frac{1}{h_i}\int_{x_{i-1/2}}^{x_{i+1/2}} \psi_m(x,y)dx \tag{6}$$

and the zero'th order x-moment of the source

$$\hat{S}_{m,i}(y) \equiv [\sigma_{S0i,j} + \frac{\nu}{k}\sigma_{Fi,j}]\sum_{n=1}^{M}\hat{\psi}_{n,i}(y)\omega_n \quad . \tag{7}$$

Equations (2) and (5) are exact; thus far, we have made no approximations. However, for each spatial node $D_{i,j}$ and together with the node boundary conditions, i.e., using estimations or prescribed values for the node incident quantities

$$\begin{cases} \tilde{\psi}_{m,j}(x_{i+1/2}) \equiv \tilde{\psi}_{m,i+1/2,j} & , \quad \mu_m < 0 \\ \tilde{\psi}_{m,j}(x_{i-1/2}) \equiv \tilde{\psi}_{m,i-1/2,j} & , \quad \mu_m > 0 \end{cases} \tag{8}$$

and

$$\begin{cases} \hat{\psi}_{m,i}(y_{j+1/2}) \equiv \hat{\psi}_{m,i,j+1/2} & , \quad \eta_m < 0 \\ \hat{\psi}_{m,i}(y_{j-1/2}) \equiv \hat{\psi}_{m,i,j-1/2} & , \quad \eta_m > 0 \end{cases}, \tag{9}$$

equations (2) and (5) form a system of 2M ordinary differential equations in 6M unknown quantities. Therefore, to obtain a unique solution, besides the node boundary conditions, given by Eqs. (8) and (9), we need to consider approximations that relate the angular flux $\psi_m(x,y)$ to its zero'th order x- and y-moments in the transverse leakage terms. In this paper we consider constant approximations for the transverse leakage terms. That is,

$$\frac{\eta_m}{k_j}[\psi_m(x, y_{j+1/2}) - \psi_m(x, y_{j-1/2})] \approx \frac{\eta_m}{k_j}(\hat{\psi}_{m,i,j+1/2} - \hat{\psi}_{m,i,j-1/2}) \equiv \hat{L}_{m,i,j} \tag{10}$$

and

$$\frac{\mu_m}{h_i}[\psi_m(x_{i+1/2},y)-\psi_m(x_{i-1/2},y)]\approx\frac{\mu_m}{h_i}(\tilde{\psi}_{m,i+1/2,j}-\tilde{\psi}_{m,i-1/2,j})\equiv\tilde{L}_{m,i,j}\,. \tag{11}$$

The general solutions of equations (2) and (5) in $D_{i,j}$ with flat approximations for the transverse leakage terms are given by

$$\tilde{\psi}_{m,j}(x)=\tilde{\psi}^{p}_{m,j}(x)+\tilde{\psi}^{h}_{m,j}(x)\quad,\quad x\in D_{i,j} \tag{12}$$

and

$$\hat{\psi}_{m,i}(y)=\hat{\psi}^{p}_{m,i}(y)+\hat{\psi}^{h}_{m,i}(y)\quad,\quad y\in D_{i,j}\,, \tag{13}$$

Here the superscript p indicates the particular solution that depends upon the approximations we make in the transverse leakage terms and the interior source $Q_{i,j}$. The superscript h indicates the homogeneous component of the solution, which satisfies the homogenous equation associated with Eqs. (2) and (5). By substituting Eq. (10) into Eq. (2), we seek for spatially constant particular solution to the resulting equation. Therefore, we obtain

$$\tilde{\psi}^{p}_{m,i,j}=\frac{Q_{i,j}}{\sigma_{Ti,j}(1-c_{0i,j})}-\frac{c_{0i,j}}{\sigma_{Ti,j}(1-c_{0i,j})}\sum_{n=1}^{M}\hat{L}_{n,i,j}\omega_n-\frac{\hat{L}_{m,i,j}}{\sigma_{Ti,j}}, \tag{14}$$

$$\text{where } c_{0,i,j}=\frac{\sigma_{s0i,j}+\frac{\nu}{k}\sigma_{fi,j}}{\sigma_{Ti,j}}\quad,\quad m=1:M\ .$$

A similar expression is obtained for the particular solution of Eq. (5). In order to obtain the homogeneous components of the general solutions, we perform a spectral analysis of the homogeneous equations associated with Eqs. (2) and (5). This spectral analysis is described in details in Ref. 6. Combining the particular solution (14) with the homogeneous solution that we obtain from the spectral analysis,

$$\tilde{\psi}^{h}_{m,j}(x) = \sum_{k=1}^{M} \beta_k \tilde{\psi}^{h}_{m,j}(x, \vartheta_k) = \sum_{k=1}^{M} \beta_k a^{x}_{m}(\vartheta_k) \exp(-\sigma_{Ti,j} x / \vartheta_k), \quad m = 1:M, \tag{15}$$

where β_k , $k = 1:M$, are arbitrary constants, we use Eq. (12) to write down the general solution of Eq. (2). To find the general solution in the y variable, given by Eq. (13), we proceed similarly.

3. NUMERICAL SCHEME

Let us integrate the one-speed X,Y-geometry S_N equations with isotropic scattering (1) over an arbitrary node $D_{i,j}$. The result is the familiar spatial balance equation

$$\frac{\mu_m}{h_i}(\tilde{\psi}_{m,i+1/2,j} - \tilde{\psi}_{m,i-1/2,j}) + \frac{\eta_m}{k_j}(\hat{\psi}_{m,i,j+1/2} - \hat{\psi}_{m,i,j-1/2}) + \sigma_{Ti,j}\overline{\psi}_{m,i,j} = (\sigma_{soi,j} + \frac{\nu\sigma_{fi,j}}{k})\sum_{n=1}^{M} \overline{\psi}_{n,i,j}\omega_n \tag{16}$$

$$m = 1:M,$$

where the node-average angular flux is defined as

$$\overline{\psi}_{m,i,j} \equiv \frac{1}{h_i k_j} \int_{x_{i-1/2}}^{x_{i+1/2}} \int_{y_{j-1/2}}^{y_{j+1/2}} \psi_m(x, y)dxdy . \tag{17}$$

The balance equation (16) combined with appropriate continuity conditions on the node edges and boundary conditions imposed on the outer boundaries of the domain form an underdetermined system; therefore we need auxiliary equations in order to obtain the same number of equations as unknowns. In the non-multiplying regions of the domain, e.g., reflector and baffle, we use the SGF auxiliary equations.[4] In the fuel regions, we use the non-standard SD auxiliary equations

$$\overline{\psi}_{m,i,j} = \sum_{n=1}^{M} \theta_{m,n}(\frac{\tilde{\psi}_{n,i-1/2,j} + \tilde{\psi}_{n,i+1/2,j}}{2}) + \hat{G}_{m,i,j} \tag{18}$$

and

$$\overline{\psi}_{m,i,j} = \sum_{n=1}^{M} \gamma_{m,n}(\frac{\hat{\psi}_{n,i,j-1/2} + \hat{\psi}_{n,i,j+1/2}}{2}) + \tilde{G}_{m,i,j}, \tag{19}$$

where $m = 1:M$. In Eq. (18) $\theta_{m,n}$ and $\hat{G}_{m,i,j}$ are determined by requiring that the general solution of Eq. (2), with flat leakage approximation, given by Eq. (15), has node-average and node-edge average angular fluxes that for all values of β_k satisfy Eq. (18). We remark that, for each estimate of the dominant eigenvalue k in the outer iterations, we need to calculate the M^2 unknowns $\theta_{m,n}$ by solving linear systems that we obtain for the cases $c_{o\,i,j} < 1$ or $c_{o\,i,j} > 1$. Following similar procedure, we obtain the expression for $\tilde{G}_{m,i,j}$ and linear systems for the M^2 constants $\gamma_{m,n}$ in Eq. (19). The balance equations (16), combined with the auxiliary equations (18) and (19) and appropriate continuity and boundary conditions form the SD-CN equations.

At this point we remark that, unlike the SGF auxiliary equations used in deep penetration S_N problems, the SD auxiliary equations relate the node-average angular fluxes to the node-edge average angular fluxes in *all* directions, including the exiting directions. This good feature of the SD auxiliary equations is convenient for multiplying media as it indicates that an interior neutron source (due to fission) exists inside node $D_{i,j}$. On the other hand, for the non-multiplying regions, e.g., baffle and reflector, we use the SGF-CN method. We note, though, that we initially used the SGF equations for the whole domain in S_N eigenvalue problems in slab geometry. However, the SGF method showed some unstability for one-dimensional coarse-mesh calculations. In two dimensions, on the other hand, this coarse-mesh unstability might be alleviated by the presence of the transverse angular fluxes in the SGF auxiliary equations. We intend to investigate this possibility in near future.

4. ITERATIVE ALGORITHM

Power method is traditionally used to converge the dominant solution of S_N eigenvalue problems. For each estimate of the dominant eigenvalue k in the outer iterations, we solve a "fixed-source" S_N problem using inner iterations. The "one-node block inversion" (NBI) scheme iterates on the node-edge average angular fluxes by performing "node-block inversions". That is, the NBI scheme uses the best estimates available for the incoming node-edge average angular fluxes to evaluate the exiting fluxes, that constitute the incoming fluxes for the adjacent nodes in the directions of the transport sweeps. To illustrate this concept, let us consider Figure 2 representing an arbitrary spatial node $D_{i,j}$ with the node-edge average angular fluxes. Each arrow in Figure 2 represents N(N+2)/8 directions in each quadrant. For the sweep indicated (from SW to NE), the outward arrows (thicker arrows) in the north and east of $D_{i,j}$ represent the outgoing node-edge average angular fluxes we need to calculate, because they form the incoming node-edge average angular fluxes for the adjacent nodes in this sweep. The inward arrows (medium arrows) represent the incoming node-edge average angular fluxes, that are known, or at least we use the best estimates available for them. Finally, the outward arrows (thinner arrows) in the south and west of $D_{i,j}$ represent the node-edge average angular fluxes, that can be calculated, but are not needed for this sweep. They represent the outgoing quantities that are needed for the NE to SW sweep. An analogous convention is followed for the NW to SE and SE

to NW transport sweeps. As we see, we need to iterate only on the node-edge average angular fluxes. As it is, unlike the conventional source iteration (SI) scheme [1], the NBI scheme needs to store the node-edge average fluxes in all directions. For coarse-mesh calculations though, this storage is very much alleviated, apart from the fact that the convergence rate of the NBI scheme is higher than the convergence rate of the SI scheme for coarse spatial grids.

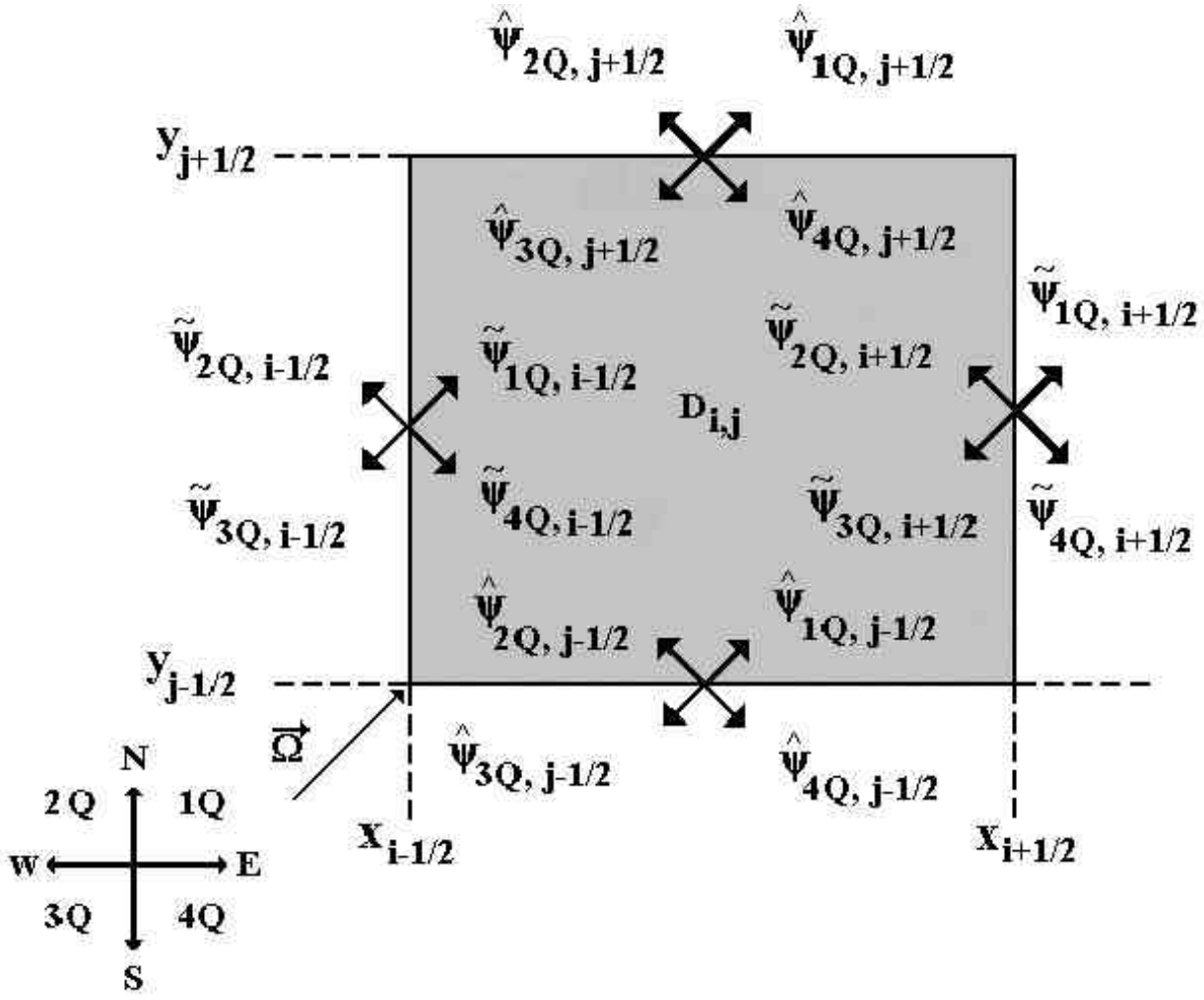

Figure 2. SW to NE transport sweep.

5. NUMERICAL RESULTS AND DISCUSSION

In this section, we perform a numerical experiment to illustrate the accuracy of the present hybrid SD-SGF-CN method for coarse-mesh nuclear reactor global calculations. Figure 3 shows 1/4 of

a two-dimensional x,y nuclear reactor core cut perpendicular to its z-axis, whose material zones have the one energy group data listed in Table I.

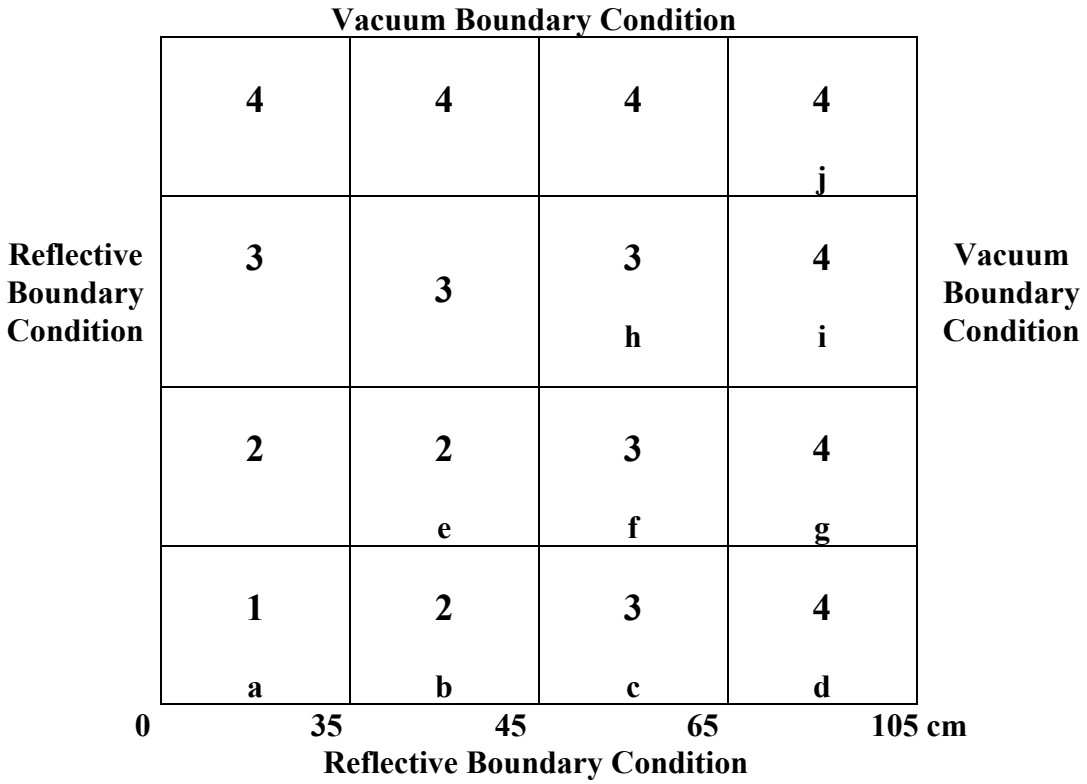

Figure 3. Model Problem (1/8 – symmetric domain)

Table I. Nuclear Data

Zone Number	σ_T	σ_{s0}	$\nu\sigma_f$
1	2.22589E-1[a]	2.20563E-1	2.83283E-3
2	2.16566E-1	2.10697E-1	1.04347E-2
3	3.01439E-1	2.96069E-1	5.13036E-4
4	2.52250E-1	2.50794E-1	0.0

[a] Read as 2.22589×10^{-1}.

Table II shows the dominant eigenvalue (effective multiplication factor - k_{eff}) generated by the conventional Constant-Constant Nodal (CCN) method [7], the conventional Linear Nodal (LN) method [5] and the present SD-SGF-CN method with the S_4 level symmetric angular quadrature set[1] on various spatial grids. The reference result has been generated by the traditional Diamond Difference (DD) method [1] on a very fine grid, composed of 64 spatial cells per region in each spatial direction (x and y).

Table II. Effective Multiplication Factor (k_{eff})

Spatial Grid Γ_n [a]	Numerical Method	k_{eff}	Relative Deviations (%) [c]
Γ_2	CCN	0.62134357	35.42
	LN	0.93844318	2.46
	SD-SGF-CN	0.96865121	0.67
Γ_3	CCN	0.77330886	19.63
	LN	0.95868309	0.37
	SD-SGF-CN	0.96395579	0.18
Γ_4	CCN	0.88168998	8.37
	LN	0.96182392	0.04
	SD-SGF-CN	0.96273334	0.06
Γ_5	CCN	0.93553854	2.77
	LN	0.96217276	0.00
	SD-SGF-CN	0.96235346	0.02
Γ_6	CCN	0.95479778	0.77
	LN	0.96220192	0.00
	SD-SGF-CN	0.96224372	0.00
Γ_7	CCN	0.96029527	0.19
	LN	0.96220398	0.00
	SD-SGF-CN	0.96221464	0.00
Γ_8	DD [b]	0.96220092	

[a] 2^n / 4 spatial nodes per region in each spatial direction.
[b] Diamond Difference method.
[c] Relative deviation with respect to the DD fine-mesh solution.

As we see, the SD-SGF-CN method is more accurate than the CCN method, although in both methods, we consider flat approximations for the transverse leakage terms and we deal only with zero'th order spatial moment transverse-integrated S_N equations. On the other hand, the SD-SGF-CN method generated numerical results for the effective multiplication factor that were about as

accurate as the LN results, except for very coarse grids, whereon the SD-SGF-CN method generated more accurate results, although in the LN method we consider linear approximations for the transverse leakage terms and we deal with zero'th and first order spatial moment transverse-integrated S_N equations. Furthermore, Figure 4 shows the relative deviations (%) of the average power density distribution within the domain represented in Figure 3, as generated by the CCN, the LN and the SD-SGF-CN methods with respect to the fine-grid reference results generated by the DD method.

			j
	***CCN **LN *SD-SGF-CN	*** 34.58 ** 11.54 * 3.27 **h**	**i**
	8.80 3.98 8.61 **e**	23.19 10.59 3.88 **f**	**g**
4.22 0.67 0.03 **a**	0.74 0.38 0.92 **b**	12.91 5.47 0.54 **c**	**d**

Figure 4. Relative deviations (%) in the average power density distribution generated on a spatial grid composed of 1 node per region (1/8 – symmetric domain).

According to Figure 4 (spatial grid composed of 1 node per region), the maximum deviation turned out to be 34.58% in region h, generated by the CCN method. On the same spatial grid, the maximum deviation generated by the LN method was 11.54% in region h and the maximum deviation generated by the SD-SGF-CN method was 8.61% in region e. As with the efficiency of the offered SD-SGF-CN method for coarse-mesh calculations, let us consider the following *gedankenexperiment*. In performing nuclear reactor global calculations, let us suppose that the user considers that relative deviations in the effective multiplication factor, greater than 5%, with respect to the reference result, are not acceptable. In this case, according to Table II, the CCN method satisfies the user's demand on a spatial grid composed of 8 x 8 nodes per region, whereas the SD-SGF-CN method satisfies the same condition on a spatial grid composed of 1 x 1 node per region. Therefore, considering that we ran both methods on the same machine with the NBI scheme in the inner iterations, it is fair to compare the CPU execution times. The CCN code generated the dominant eigenvalue within 2.77% in 3484 seconds. This is in contrast to the SD-SGF-CN code that generated the dominant eigenvalue within 0.67% in 43 seconds. As the LN code has been implemented with a different iterative scheme, i.e., the SI scheme, we do not think

it is fair to compare execution time of the LN code with the execution times of the CCN and SD-SGF-CN codes at the moment. Before closing, we list a number of general conclusions and suggestions for future work: (i) the SD-SGF-CN method, as described in this paper, is much more accurate than the conventional CCN method for coarse-mesh calculations, although in both methods we consider flat leakage approximations; (ii) the SD-SGF-CN method generated numerical results for this test problem that were, roughly speaking, as accurate as the LN results. However, this good feature seems to be problem dependent, and for future work, we suggest to develop the companion SD-SGF-LN method, and compare it more fairly with the LN method; (iii) we also suggest to extend the present one-speed SD-SGF-CN method to multigroup S_N problems, and this should be quite straightforward.[2] Moreover, the extension to three-dimensional S_N problems with linearly anisotropic scattering should not add a great deal of theoretical difficulties.

ACKNOWLEDGMENTS

This work was developed by the Deterministic Computational Neutronics (DCN) research team, sponsored by CNPq – Brazil. The authors acknowledge the fruitful help provided by Marcos Pimenta de Abreu (IPRJ/UERJ – DCN), José Humberto Zani (IPRJ/UERJ – DCN), Todd Wareing (LANL) and Yousry Azmy (ORNL) during the development of this work.

REFERENCES

1. E. E. Lewis and W. F. Miller Jr., *Computational Methods of Neutron Transport*, John Wiley and Sons, NY, 1984.

2. M. P. de Abreu, H. Alves Filho and R. C. Barros, *Transport Theory and Statistical Physics*, **25** (1), 61, 1996.

3. H. Alves Filho, F. C. da Silva and R. C. Barros, *Int. Conf. on the Physics of Nuc. Sci. and Tech*., Proceedings Vol. 1, 515, USA, 1998 .

4. R. C. Barros and E. W. Larsen, *Nucl. Sci. Eng.*, **111**, 34, 1992.

5. W. F. Walters, *Progress in Nuclear Energy*, **18**, 21, 1986.

6. R. C. Barros, F. C. da Silva and H. Alves Filho, *Progress in Nuclear Energy*, **18**, 21, 1986.

7. W. F. Walters and R. D. O'Dell, ANS/ENS Int. Top. Meeting on Adv. in Math. Meth. for Solution of Nuc. Eng. Prob., **1**, 114, Germany, 1981.